

# Half-life and spin of $^{60}\text{Mn}^g$

S.N. Liddick<sup>1,2</sup>, P.F. Mantica<sup>1,2</sup>, B.A. Brown<sup>1,3</sup>, M.P. Carpenter<sup>4</sup>, A.D. Davies<sup>1,3</sup>,  
M. Horoi<sup>5</sup>, R.V.F. Janssens<sup>4</sup>, A.C. Morton<sup>1</sup>, W.F. Mueller<sup>1</sup>, J. Pavan<sup>6</sup>,  
H. Schatz<sup>1,3</sup>, A. Stolz<sup>1</sup>, S.L. Tabor<sup>6</sup>, B.E. Tomlin<sup>1,2</sup>, M. Wiedeking<sup>6</sup>

<sup>(1)</sup> *National Superconducting Cyclotron Laboratory,*

*Michigan State University, East Lansing, Michigan 48824*

<sup>(2)</sup> *Department of Chemistry, Michigan State University, East Lansing, Michigan 48824*

<sup>(3)</sup> *Department of Physics and Astronomy,*

*Michigan State University, East Lansing, Michigan 48824*

<sup>(4)</sup> *Physics Division, Argonne National Laboratory, Argonne, Illinois 60439*

<sup>(5)</sup> *Department of Physics, Central Michigan University,*

*Mount Pleasant, Michigan 48859 and*

<sup>(6)</sup> *Department of Physics, Florida State University, Tallahassee, Florida 32306*

(Dated: March 24, 2006)

## Abstract

A value of  $0.28 \pm 0.02$  s has been deduced for the half-life of the ground state of  $^{60}\text{Mn}$ , in sharp contrast to the previously adopted value of  $51 \pm 6$  s. Access to the low-spin  $^{60}\text{Mn}$  ground state was accomplished via  $\beta$  decay of the  $0^+$   $^{60}\text{Cr}$  parent nuclide. New, low-energy states in  $^{60}\text{Mn}$  have been identified from  $\beta$ -delayed  $\gamma$ -ray spectroscopy. The new, shorter half-life of  $^{60}\text{Mn}^g$  is not suggestive of isospin forbidden  $\beta$  decay, and new spin and parity assignments of  $1^+$  and  $4^+$  have been adopted for the ground and isomeric  $\beta$ -decaying states, respectively, of  $^{60}\text{Mn}$ .

## INTRODUCTION

The nuclide  $^{60}\text{Mn}$  has two known  $\beta$ -decaying states.  $\beta$  decay of a proposed  $3^+$  level was initially established by Norman *et al.* [1], and a half-life of  $1.79 \pm 10$  s was reported together with several delayed  $\gamma$ -ray transitions depopulating excited states in the  $^{60}\text{Fe}$  daughter nuclide. Subsequently, Runte *et al.* [2] deduced that the  $3^+$  level was isomeric, decaying with an internal transition (IT) to  $\beta$  ratio of  $0.13 \pm 0.01$ . A 272-keV  $\gamma$  ray, with a decay half-life of 1.8 s, was designated as the IT, and  $M3$  multipolarity was assigned based on Weisskopf estimates. Additional  $\beta$ -delayed  $\gamma$  rays were identified by Runte *et al.*, including a 1150-keV transition known to depopulate the first excited  $0^+$  state in  $^{60}\text{Fe}$ . The first measurement of the half-life of the presumed  $0^+$  ground state of  $^{60}\text{Mn}$  was completed by Bosch *et al.* [3]. A half-life of  $51 \pm 6$  s was deduced from the multiscaled  $\beta$  singles counting rate. No evidence was found in their work for delayed  $\gamma$  rays following  $\beta$  decay of the  $^{60}\text{Mn}$  ground state. The long half-life value for the ground-state  $\beta$  decay of  $^{60}\text{Mn}$ , in combination with the apparent direct feeding of the daughter  $^{60}\text{Fe}$  ground state, resulted in a  $\log ft$  value of 6.7, suggesting an isospin-forbidden Fermi decay of the  $^{60}\text{Mn}$  ground state. Several examples of isospin-forbidden  $0^+ \rightarrow 0^+$  transitions are known [4], all having  $\log ft > 6.5$ . Therefore, the  $^{60}\text{Mn}$  ground-state  $\beta$  decay was identified as a potential candidate for isospin-forbidden  $\beta$  decay.

Doubt regarding the long half-life of  $^{60}\text{Mn}^g$  was reported by Schmidt-Ott *et al.* [5], who set out to directly measure the multipolarity of the IT in both  $^{58,60}\text{Mn}$  using conversion electron spectroscopy. At  $A = 60$ , the  $M3$  multipolarity assignment to the 272-keV  $\gamma$  ray was confirmed based on the measured  $\alpha_K$  value. However, multiscaled  $\beta$  singles measurements showed a long-lived  $45.5 \pm 1.7$  s activity at  $A = 60$  that was associated with the decay of two known isomers in  $^{120}\text{In}$  [6]. The In activity was present as a doubly-ionized species from the ion source of the on-line mass separator and appeared at  $A = 60$  due to its having an identical  $m/q$  ratio. The initial half-life measurement of the  $^{60}\text{Mn}$  ground state by Bosch *et al.* [3] was also carried out using on-line mass separation and a possible contamination of the  $^{60}\text{Mn}$   $\beta$  spectrum from  $^{120}\text{In}^{2+}$  cannot be ruled out.

We report a new measurement of the  $\beta$ -decay half-life of the  $^{60}\text{Mn}$  ground state. To eliminate contributions from the  $^{60}\text{Mn}$  isomeric-state  $\beta$  decay, we selectively populated the  $^{60}\text{Mn}$  ground state following the  $\beta$  decay of the even-even  $^{60}\text{Cr}$  ground state, with  $J^\pi = 0^+$

and two independently determined half-lives of  $0.57 \pm 0.06$  s [3] and  $0.51 \pm 0.15$  s [7].

## EXPERIMENTAL METHODS

The parent  $^{60}\text{Cr}$  activity was produced following projectile fragmentation of a 140-MeV/nucleon  $^{86}\text{Kr}$  beam at the National Superconducting Cyclotron Laboratory at Michigan State University. The  $^{86}\text{Kr}$  primary beam, with an average beam current of 15 pA, was incident onto a  $376\text{-mg/cm}^2$  thick Be target located at the object position of the A1900 fragment separator [8]. The secondary fragments of interest, including  $^{60}\text{Cr}$ , were selected in the A1900 separator using a  $330\text{ mg/cm}^2$  Al degrader and 1% momentum slits; both were located at the intermediate image of the device. The dipole magnets of the A1900 fragment separator were set to magnetic rigidities  $B\rho_1 = 4.239$  Tm and  $B\rho_2 = 3.944$  Tm. These same settings were used in the previously reported  $\beta$ -decay studies of  $^{56}\text{Sc}$  [9] and  $^{57}\text{Ti}$  and  $^{59}\text{V}$  [10].

The fully-stripped  $^{60}\text{Cr}$  fragments, along with  $^{56}\text{Sc}$ ,  $^{57}\text{Ti}$ , and  $^{58,59}\text{V}$  were implanted in a Double-Sided Si microstrip Detector (DSSD) with thickness  $1470\ \mu\text{m}$  that is part of the NSCL  $\beta$  counting system [11]. Fragments were unambiguously identified by a combination of multiple energy loss signals and time of flight. A total of  $2.75 \times 10^5$   $^{60}\text{Cr}$  ions, composing 24% of the secondary beam, were implanted into the DSSD.

Fragment- $\beta$  correlations were established in software by requiring a high-energy implantation event in a single pixel of the DSSD, followed by a low-energy  $\beta$  event in the same or any of the eight nearest-neighbor pixels. The differences between the absolute time stamps of correlated  $\beta$  and implantation events were histogrammed to generate decay curves. To suppress background, implantation events were rejected if they were not followed by a  $\beta$  event within 5 s, or if they were followed by a second implantation within the same 5 s time interval. The  $\beta$ -detection efficiency was  $\sim 30\%$ . Delayed  $\gamma$  rays were measured with 12 detectors from the MSU Segmented Germanium Array [12] arranged around the  $\beta$  counting system. The  $\gamma$ -ray peak detection efficiency was 5.3% at 1 MeV. The energy resolution for each of the Ge detectors was  $\sim 3.5$  keV for the 1.3 MeV  $\gamma$ -ray transition in  $^{60}\text{Co}$ . Additional details regarding the  $\beta$ -delayed  $\gamma$ -ray techniques used with fast fragmentation beams at the NSCL are available in Ref. [13].

## RESULTS AND DISCUSSION

The decay curve for  $\beta$  events that occurred within 5 s of a  $^{60}\text{Cr}$  implantation event is shown in Fig. 1(a). From the shape of the decay curve below 100 ms, it is apparent that the daughter  $^{60}\text{Mn}$  has a shorter half-life than  $^{60}\text{Cr}$ . The decay curve of Fig. 1(a) was fitted with a function that considered the exponential decay of the  $^{60}\text{Cr}$  parent, the exponential growth and decay of the  $^{60}\text{Mn}$  daughter, and a linear background. A half-life value of  $0.49 \pm 0.01$  s was deduced for the  $^{60}\text{Cr}$  parent, in reasonable agreement with previous measurements by Bosch *et al.* [3]  $0.57 \pm 0.06$  s and Dörfler *et al.* [7]  $0.51 \pm 0.15$  s. A half-life value of  $0.28 \pm 0.02$  s was deduced for the  $^{60}\text{Mn}$  ground-state, in stark contrast to the long half-life of  $51 \pm 6$  s deduced by Bosch *et al.* [3].

The  $\beta$ -delayed  $\gamma$ -ray spectrum for events that occurred within 1 s of a  $^{60}\text{Cr}$  implantation event within the DSSD is given in Fig. 2.  $\gamma$  rays evident in this spectrum correspond to short-lived  $\beta$ -decay events. Since the ground states of both  $^{60}\text{Cr}$  and  $^{60}\text{Mn}$  were found to have half-life values of less than 1 s, their corresponding delayed  $\gamma$  rays should be present in this spectrum. The assignment of  $\gamma$ -ray transitions to either the parent or daughter decay was accomplished by analysis of the fragment- $\beta\gamma$  decay curves. The 823-keV  $\gamma$  ray had been previously assigned to the deexcitation of the first excited  $2^+$  state in  $^{60}\text{Fe}$ . The fragment- $\beta\gamma$  decay curve for this transition, illustrated in Fig. 1(c), exhibits the growth of  $^{60}\text{Mn}^g$  (from the  $^{60}\text{Cr}$  parent decay) as well as its presently-determined  $T_{1/2} = 0.28$  s decay. The decay curves gated on the delayed  $\gamma$  rays with energies 1150 and 1532 keV showed similar structure and have also been assigned in the present work to the deexcitation of levels in  $^{60}\text{Fe}$ . The other three delayed  $\gamma$ -ray transitions in Fig. 2 all reveal half-lives consistent with the decay of the  $^{60}\text{Cr}$  parent. As an example, the  $\gamma$ -ray gated decay curve derived for the 349-keV transition is presented in Fig. 1(b). The three transitions with energies 349, 410, and 758 keV have, in the present work, been identified as depopulating excited states in  $^{60}\text{Mn}$ .

The new half-life value of  $0.28 \pm 0.02$  s for the decay of  $^{60}\text{Mn}^g$  is not consistent with the  $0^+$  spin and parity quantum numbers previously assigned to the  $^{60}\text{Mn}$  ground state. Such a short half-life and direct  $\beta$ -decay feeding to the  $^{60}\text{Fe}$  ground state would purport a large  $B(\text{Fermi})$  value that is unexpected for an isospin-forbidden  $0^+ \rightarrow 0^+$  Fermi transition. A review of the experimental basis for the spin and parity assignments to the ground and isomeric states in  $^{60}\text{Mn}$ , therefore, is warranted. The  $\Delta J = 3$  spin difference between the

ground and isomeric states is firmly established by the conversion electron measurements of Schmidt-Ott *et al.* [5]. However, the initial  $3^+$  spin and parity assignment to the isomeric state can be called into question, since this assignment is based solely on the apparent  $\log ft$  values indicating allowed  $\beta$  decays to the  $2_2^+$ ,  $3_1^+$  and  $4_1^+$  states in  $^{60}\text{Fe}$  [1]. The absolute  $\beta$  intensity to the  $2_2^+$  level in  $^{60}\text{Fe}$  was reported to be  $(6.7 \pm 2.0)\%$ , but with a large  $Q_\beta$  value window of 8.2 MeV [14] this apparent  $\beta$  feeding should only be considered an upper limit since the presence of unobserved transitions from higher-energy states in  $^{60}\text{Fe}$  cannot be ruled out [15]. An assignment of  $J^\pi = 4^+$ , therefore, cannot be excluded for the  $^{60}\text{Mn}$  isomeric state. The adoption of  $J^\pi = 4^+$  for  $^{60}\text{Mn}^m$  would also change the proposed ground state spin and parity of  $^{60}\text{Mn}$  to  $J^\pi = 1^+$  due to the known  $M3$  multipolarity for the 272-keV IT between the two states. The apparent direct  $\beta$ -decay feeding to the ground and two excited  $0^+$  states in  $^{60}\text{Fe}$  (see below) would be consistent with allowed Gamow-Teller decay if the parent state had  $J^\pi = 1^+$ .

To further support the proposed changes in the spin and parity assignments of  $1^+$  and  $4^+$  to the ground and isomeric states of  $^{60}\text{Mn}$ , respectively, the low-energy levels of this nuclide were calculated in the full  $pf$ -shell model space with the GXPF1 interaction [16, 17]. This interaction is derived from a microscopic calculation based on renormalized G matrix theory with the Bonn-C interaction and refined by a systematic adjustment of the important linear combinations of two-body matrix elements to low-lying states in nuclei from  $A = 47$  to  $A = 66$ . The GXPF1 interaction has met with success in describing the  $\beta$ -decay properties and low-energy levels of the neutron-rich  $\pi f_{7/2} - \nu pf$  shell nuclei [9, 10, 13, 18]. The OXBASH [19] and CMICHSM [20] codes were used to generate the results for  $^{60}\text{Mn}$  shown in Fig. 3. The ground state is predicted to have  $J^\pi = 1^+$ , and the first  $4^+$  level is calculated at 224 keV. The first  $J^\pi = 0^+$  level is expected at an energy more than 1.4 MeV above the ground state. The wavefunctions of the lowest-energy  $1^+$  and  $4^+$  states are predominately associated with the  $\pi(f_{7/2}) - \nu(f_{5/2})$  multiplet. In retrospect, the coupling scheme which would produce a  $0^+$  state from the shell model orbitals expected to be occupied by the valence protons and neutrons in  $^{60}\text{Mn}$  is not obvious; the  $\pi(f_{7/2})$  orbital is half-filled and valence neutrons should occupy the  $p_{1/2}$  and  $f_{5/2}$  orbitals so that  $j_p - j_n = 0$  is not possible [21, 22].

Shell model calculations were also completed in a similar manner for  $^{58}\text{Mn}$ . Bosch *et al.* [3] initially proposed  $J^\pi = 0^+$  for the ground state of  $^{58}\text{Mn}$ . However, the small comparative

half-life (apparent  $\log ft$  value of 4.9) for direct decay to the  $0^+$  ground state of the  $^{58}\text{Cr}$  was not suggestive of isospin-forbidden  $\beta$  decay. The results of the shell model calculations in the full  $pf$ -shell model space suggest that the first  $0^+$  state should reside more than 1.5 MeV above the ground state (see Fig. 3.) Indeed, spin and parity of  $1^+$  have been adopted for the  $^{58}\text{Mn}$  ground state in the most recent data compilation [23]. The calculated ground and first excited states, with  $J^\pi = 4^+$  and  $1^+$ , respectively, are separated in energy by 75 keV. Experimentally, these states are observed in reverse order and with a similar energy separation of 72 keV. The order of states separated by such a small energy difference cannot be accurately predicted by the GXPF1 interaction, which has an *rms* error of 168 keV [17]. However, the calculated  $\beta$  decay half-life of 2.75 s for the lowest  $1^+$  level in  $^{58}\text{Mn}$  is in good agreement with the experimental half-life value of  $3.0 \pm 0.1$  s [24] of  $^{58}\text{Mn}^g$ , suggesting that the adopted order of states, with  $1^+$  as the ground state and  $4^+$  as the first excited state, is correct.

Further details regarding the  $\beta$ -decay properties of both  $^{60}\text{Cr}$  and  $^{60}\text{Mn}^g$  are given in Fig. 4 and Fig. 5, respectively. For  $^{60}\text{Cr}$ , a new half-life value of  $0.49 \pm 0.01$  s was deduced from the decay curves gated on the  $\gamma$ -ray transitions with energies of 349, 410, and 758 keV. This value agrees with previously-reported half-life values of  $0.57 \pm 0.06$  s [3] and  $0.51 \pm 0.15$  s [7]. The 349- and 410-keV  $\gamma$  rays are coincident; however, the ordering of the two transitions in the level scheme of  $^{60}\text{Mn}$  cannot be resolved by the present data set. The 758-keV  $\gamma$  ray is the sum energy of the 349- and 410-keV transitions and has been placed as directly feeding the  $^{60}\text{Mn}$  ground state. The majority of the  $\beta$  decay of  $^{60}\text{Cr}$  directly populates the  $^{60}\text{Mn}$  ground state. Apparent  $\beta$  branching to the two new excited levels in  $^{60}\text{Mn}$  is also observed, but the feeding intensities quoted in Fig. 4 should be considered as upper limits, since the  $Q_\beta$  window is large and possible unobserved transitions depopulating into these excited states could reduce the apparent feedings. Tentative spin and parity values of  $1^+$  and  $2^+$  have been assigned to the 759-keV and 349-keV levels, respectively, based on the  $\beta$  feeding patterns and the correspondence with the shell model results presented in Fig. 3 and Table I.

Previous studies of the  $\beta$ -decay of  $^{60}\text{Mn}^g$  suggested that no excited states were populated with any significant  $\beta$  intensity [3]. Three delayed  $\gamma$  rays have been assigned in this work to the decay of  $^{60}\text{Mn}^g$  with energies 823, 1150, and 1532 keV. The  $\gamma$ -ray line at 823 keV had previously been assigned to the  $2_1^+ \rightarrow 0_1^+$  transition in  $^{60}\text{Fe}$ . The other two  $\gamma$  rays with

energies 1150 and 1532 keV are proposed to depopulate the  $0_2^+$  and  $0_3^+$  states, respectively. The two excited  $0^+$  states were previously known from transfer reaction work, and the  $J = 0$  assignment is based on  $\ell = 0$  two-neutron transfer to the  $^{58}\text{Fe}$  target [25]. A 1150-keV  $\gamma$  ray was similarly identified as deexciting the 1974-keV  $0_2^+$  level based on a study of the  $^{58}\text{Fe}(t,p\gamma)$  reaction by Warburton *et al.* [26]. While Runte *et al.* [2] observed the 1150-keV  $\gamma$  ray when studying the  $\beta$  decay of the now-adopted  $4^+$  isomeric state in  $^{60}\text{Mn}$ , it is plausible that they unknowingly monitored a mixture of both the high- and low-spin  $\beta$ -decaying states.

The branching ratios for both the  $^{60}\text{Cr}$  and  $^{60}\text{Mn}^g$   $\beta$  decay were also calculated in the full  $pf$ -shell model space with the GXPF1 interaction and the CMICHSM code [20]. There is excellent agreement between the experimental observations and the shell model results in both instances, as seen from Table I. The predicted half-lives take into consideration a quenching factor of 0.7 for the Gamow-Teller strength in this region [27]. Ground state  $\beta$  decay dominates the decay pathway for both parent and daughter nuclides, which corroborates the experimental observations.

## SUMMARY

A new half-life value of  $0.28 \pm 0.02$  s has been deduced for the ground state of  $^{60}\text{Mn}$ , which is significantly shorter than the previously adopted value of  $51 \pm 6$  s. The prospect of isospin-forbidden  $0^+ \rightarrow 0^+$  Fermi  $\beta$  decay for the  $^{60}\text{Mn}$  ground state has been ruled out by the new, short half-life value. New spin and parity assignments of  $1^+$  and  $4^+$  have been adopted for the ground and the isomeric  $\beta$ -decaying states in  $^{60}\text{Mn}$ , respectively, supported by the deduced  $\beta$ -decay properties reported here and by the results of shell model calculations using the GXPF1 interaction in the full  $pf$ -shell model space. Two new low-energy levels have been identified in  $^{60}\text{Mn}$  and evidence for direct  $\beta$  feeding of excited  $0^+$  states in  $^{60}\text{Fe}$  is reported for the first time.

The work was supported in part by the National Science Foundation Grants PHY-01-10253, PHY-97-24299, PHY-01-39950, and PHY-02-44453, and by the US Department of Energy, Office of Nuclear Physics, under contract W-31-109-ENG-38. The authors would like to thank the NSCL operations staff for providing the primary and secondary beams for this experiment. The authors also thank the members of the NSCL  $\gamma$  group who helped with the set up of the Segmented Germanium Array. The DSSD used for these measurements

was provided by K. Rykaczewski (ORNL). The shell model calculations were performed on the computer systems provided by the High Performance Computing Center at Michigan State University.

- 
- [1] E.B. Norman, C.N. Davids, M.J. Murphy, and R.C. Pardo, *Phys. Rev. C* **17**, 2176 (1978).
  - [2] E. Runte, K.-L. Gippert, W.-D. Schmidt-Ott, P. Tidemand-Petersson, L. Ziegeler, R. Kirchner, O. Klepper, P.O. Larsson, E. Roeckl, D. Schardt, N. Kaffrell, P. Peuser, M. Bernas, P. Dessagne, M. Langevin, and K. Rykaczewski, *Nucl. Phys.* **A441**, 237 (1985).
  - [3] U. Bosch, W.-D. Schmidt-Ott, E. Runte, P. Tidemand-Petersson, P. Koschel, F. Meissner, R. Kirchner, O. Klepper, E. Roeckl, K. Rykaczewski, and D. Schardt, *Nucl. Phys.* **A477**, 89 (1988).
  - [4] S. Raman and N.B. Gove, *Phys. Rev. C* **7**, 1995 (1973).
  - [5] W.-D. Schmidt-Ott, K. Becker, U. Bosch-Wicke, T. Hild, F. Meissner, R. Kirchner, E. Roeckl, and K. Rykaczewski, *Proc. 6th Intern. Conf. on Nuclei Far from Stability and 9th Intern. Conf. on Atomic Masses and Fundamental Constants*, Bernkastel-Kues, Germany, R. Neugart, A. Wöhr, Eds. p.627 (1993).
  - [6] H.C. Cheung, H. Huang, B.N. Subba Rao, L. Lessard, and J.K.P. Lee, *J. Phys. G* **4**, 1501 (1978).
  - [7] T. Dörfler, W.-D. Schmidt-Ott, T. Hild, T. Mehren, W. Böhmer, P. Möller, B. Pfeiffer, T. Rauscher, K.-L. Kratz, O. Sorlin, V. Borrel, S. Grévy, D. Guillemaud-Mueller, A.C. Mueller, F. Pougheon, R. Anne, M. Lewitowicz, A. Ostrowsky, M. Robinson, and M.G. Saint-Laurent, *Phys. Rev. C* **54**, 2894 (1996).
  - [8] D.J. Morrissey, B.M. Sherrill, M. Steiner, A. Stolz, and I. Wiedenhöver, *Nucl. Instrum. Methods Phys. Res. B* **204**, 90 (2003).
  - [9] S.N. Liddick, P.F. Mantica, R. Broda, B.A. Brown, M.P. Carpenter, A.D. Davies, B. Fornal, T. Glasmacher, D.E. Groh, M. Honma, M. Horoi, R.V.F. Janssens, T. Mizusaki, D.J. Morrissey, A.C. Morton, W.F. Mueller, T. Otsuka, J. Pavan, H. Schatz, A. Stolz, S.L. Tabor, B.E. Tomlin, and M. Wiedeking, *Phys. Rev. C* **70**, 064303 (2004).
  - [10] S.N. Liddick, P.F. Mantica, R. Broda, B.A. Brown, M.P. Carpenter, A.D. Davies, B. Fornal, M. Horoi, R.V.F. Janssens, A.C. Morton, W.F. Mueller, J. Pavan, H. Schatz, A. Stolz,



- S.L. Tabor, B.E. Tomlin, and M. Wiedeking Phys. Rev. C **72**, 054321 (2005).
- [11] J.I. Prisciandaro, A.C. Morton, and P.F. Mantica, Nucl. Instrum. Methods Phys. Res. A **505**, 140 (2003).
- [12] W.F. Mueller, J.A. Church, T. Glasmacher, D. Gutknecht, G. Hackman, P.G. Hansen, Z. Hu, K.L. Miller, P. Quirin, Nucl. Instrum. Methods Phys. Res. A **466**, 492 (2001).
- [13] P.F. Mantica, A.C. Morton, B.A. Brown, A.D. Davies, T. Glasmacher, D.E. Groh, S.N. Liddick, D.J. Morrissey, W.F. Mueller, H. Schatz, A. Stolz, S.L. Tabor, M. Honma, M. Horoi, and T. Otsuka, Phys. Rev. C **67**, 014311 (2003).
- [14] G. Audi, A.H. Wapstra, and C. Thibault, Nucl. Phys. **A729**, 337 (2003).
- [15] J.C. Hardy, L.C. Carraz, B. Jonson, and P.G. Hansen, Phys. Lett. **71B**, 307 (1977).
- [16] M. Honma, T. Otsuka, B.A. Brown, and T. Mizusaki, Phys. Rev. C **65**, 061301(R) (2002).
- [17] M. Honma, T. Otsuka, B.A. Brown, and T. Mizusaki, Phys. Rev. C **69**, 034335 (2004).
- [18] R.V.F. Janssens, B. Fornal, P.F. Mantica, B.A. Brown, R. Broda, P. Bhattacharyya, M.P. Carpenter, M. Cinausero, P.J. Daly, A.D. Davies, T. Glasmacher, Z.W. Grabowski, D.E. Groh, M. Honma, F.G. Kondev, W. Krolas, T. Lauritsen, S.N. Liddick, S. Lunardi, N. Marginean, T. Mizusaki, D.J. Morrissey, A.C. Morton, W.F. Mueller, T. Otsuka, T. Pawlat, D. Seweryniak, H. Schatz, A. Stolz, S.L. Tabor, C.A. Ur, G. Viesti, I. Wiedenhoever, and J. Wrzesinski, Phys. Lett. B **546**, 55 (2002).
- [19] B.A. Brown, A. Etchegoyen and W.D.M. Rae, The computer code OXBASH, MSU-NSCL Report No. 524, 1998.
- [20] M. Horoi, B.A. Brown, and V. Zelevinsky, Phys. Rev. C **67**, 034303 (2003).
- [21] L. Nordheim, Rev. Mod. Phys. **23**, 322 (1951).
- [22] M.H. Brennan and A.M. Bernstein, Phys. Rev. **120**, 927 (1960).
- [23] M.R. Bhat, Nucl. Data Sheets **80**, 789 (1997).
- [24] T.E. Ward, P.H. Pile, and P.K. Kuroda, Phys. Rev. **182**, 1186 (1969).
- [25] D.L. Watson and H.T. Fortune, Nucl. Phys. **A448**, 221 (1986).
- [26] E.K. Warburton, J.W. Olness, A.M. Nathan, J.J. Kolata, and J.B. McGrory, Phys. Rev. C **16**, 1027 (1977).
- [27] A. Poves, J. Sanchez-Solano, E. Caurier, and F. Nowacki, Nucl. Phys. **A694**, 157 (2001).

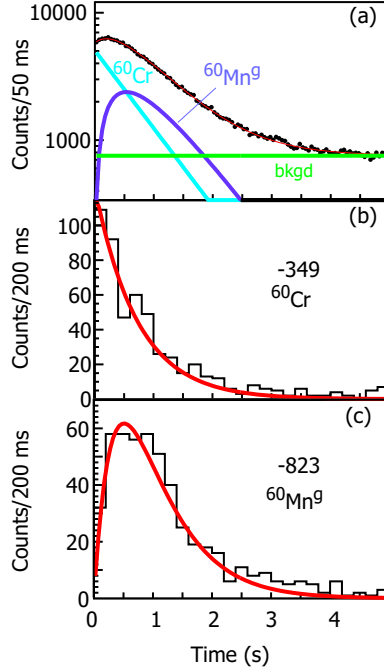


FIG. 1: (Color online) (a) Decay curve for  $^{60}\text{Cr}$  from fragment- $\beta$  correlations. The data were fitted with an exponential parent decay, an exponential daughter growth and decay, and a linear background. The decay curves for fragment- $\beta\gamma$  correlations with gates on  $\gamma$ -ray transitions with energies 349 and 823 keV are shown in (b) and (c), respectively.

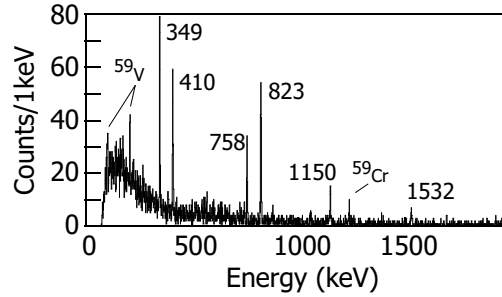


FIG. 2: Delayed  $\gamma$ -ray spectrum for  $\beta$ -decay events that occurred within 1 s of a  $^{60}\text{Cr}$  implantation event. Peaks are marked by their transition energy in keV. Contaminant lines from the  $A = 59$  decay chain were also observed due to some overlap in the particle identification spectrum.

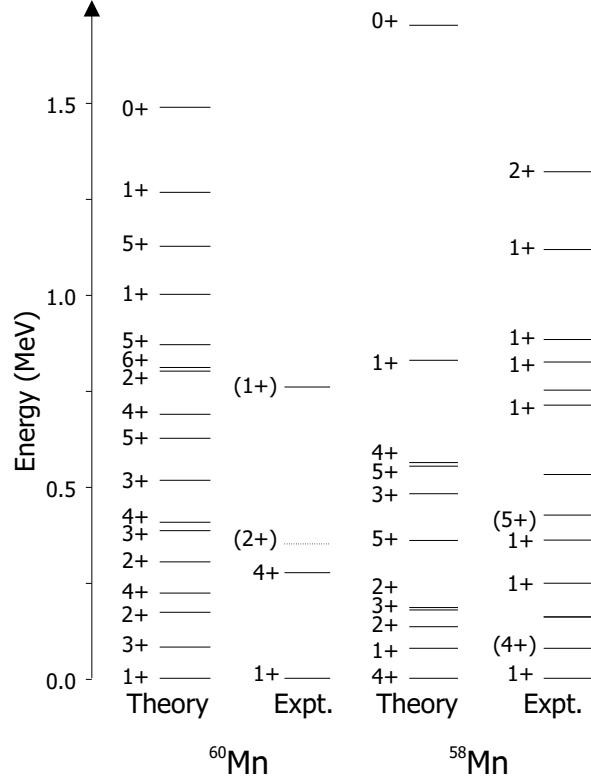


FIG. 3: Comparison of the known low-energy level structure of  $^{58}\text{Mn}$  and  $^{60}\text{Mn}$  with the results of shell model calculations in the full  $pf$ -shell model space using the GXPF1 interaction. Only the shell model results for the first three (two) states for each spin and parity up to  $J^\pi = 5^+$  for  $^{60}\text{Mn}$  ( $^{58}\text{Mn}$ ) are shown. Experimental results for  $^{58}\text{Mn}$  are taken from Ref. [23], while the data for  $^{60}\text{Mn}$  are from the present work.

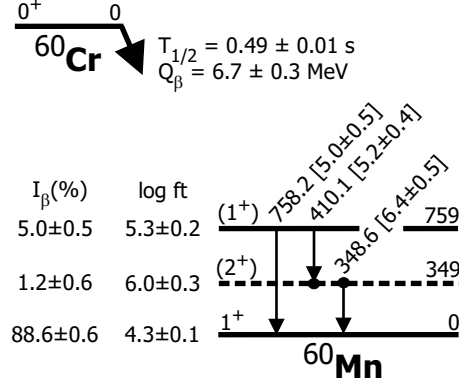


FIG. 4: Partial level scheme for  $^{60}\text{Mn}$  populated following the  $\beta$  decay of  $^{60}\text{Cr}$ . The number in brackets following a  $\gamma$ -ray transition energy is the absolute  $\gamma$ -ray intensity. The  $Q$  value was deduced from data in Ref. [14]. Observed coincidences are represented as filled circles. Absolute  $\beta$ -decay intensities and apparent  $\log ft$  values to each state in  $^{60}\text{Mn}$  are given on the left-hand side of the figure. The 349-keV level is dashed only because of the uncertainty in the ordering of the 348.6- and 410.1-keV  $\gamma$  rays. This level could instead be at 410 keV.

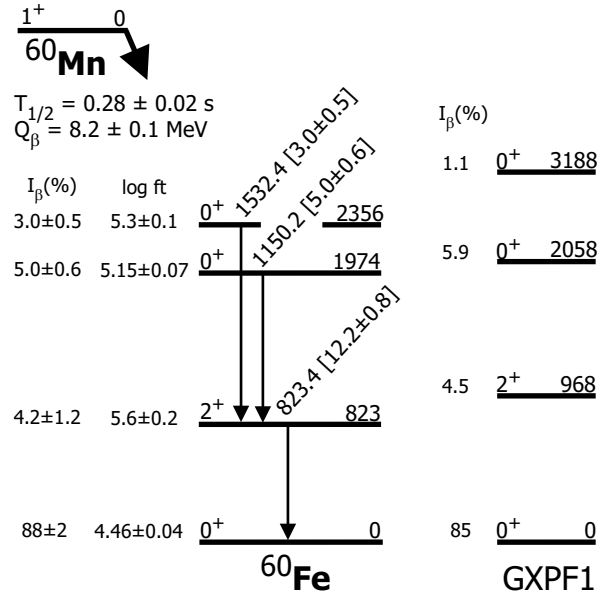


FIG. 5: Partial level scheme for  $^{60}\text{Fe}$  populated following the  $\beta$  decay of  $^{60}\text{Mn}^g$ . The number in brackets following a  $\gamma$ -ray transition energy is the relative  $\gamma$ -ray intensity. The  $Q$  value was deduced from data in Ref. [14]. Apparent  $\beta$  feedings and  $\log ft$  values are given to the left of the proposed level scheme. The results of shell model calculations using the GXPF1 interaction are presented to the right of the experimental level scheme.

TABLE I: Calculated  $\beta$ -decay branching ratios for the ground-state decays of  $^{60}\text{Cr}$  and  $^{60}\text{Mn}$ . Details regarding the shell model calculations in the full  $pf$  shell with the GXPF1 interaction are given in the text.

$^{60}\text{Cr} (0^+) \rightarrow ^{60}\text{Mn}$				$^{60}\text{Mn} (1^+) \rightarrow ^{60}\text{Fe}$			
$E_f(\text{keV})$	$J_f^\pi$	$I_\beta^{expt.}(\%)$	$I_\beta^{theory}(\%)$	$E_f(\text{keV})$	$J_f^\pi$	$I_\beta^{expt.}(\%)$	$I_\beta^{theory}(\%)$
0	$1^+$	$88.6 \pm 0.6$	91.3	0	$0^+$	$88 \pm 2$	85
(349)	$(2^+)$	$1.2 \pm 0.6$		823	$2^+$	$4.2 \pm 1.2$	4.5
758	$(1^+)$	$5.0 \pm 0.5$	3.6	1974	$0^+$	$5.0 \pm 0.6$	5.9
				2356	$0^+$	$3.0 \pm 0.5$	1.1
Sum			94.9	Sum			96.5
$T_{1/2}^{expt.}$		$0.49 \pm 0.01 \text{ s}$				$0.28 \pm 0.02 \text{ s}$	
$T_{1/2}^{theory}$		0.25 s				0.21 s	